

# Change in Piezoelectric Boundary Acoustic Wave Characteristics with Overlay and Metal Grating Materials

Yiliu Wang, Ken-ya Hashimoto, Tatsuya Omori and Masatsune Yamaguchi  
Graduate School of Engineering, Chiba University, Chiba 263-8522, Japan  
wangyiliu99@graduate.chiba-u.jp

**Abstract**— This paper describes how the propagation characteristics of shear-horizontal (SH) type piezoelectric boundary acoustic waves (PBAWs) change with overlay and metallic grating materials. We theoretically investigated the PBAW characteristics for various combinations of the overlay and metallic grating materials, and attempted to validate the qualitative prediction previously discussed and find the possible best material combination. The results are in agreement with the qualitative prediction. That is, large electromechanical coupling factor  $K^2$  is obtained when materials having small mass densities  $\rho$  and materials having extremely large  $\rho$  shear modulus  $c_{44}$  are chosen, respectively, for overlay and metallic grating. When YX-LiNbO<sub>3</sub> is assumed as a substrate, for example, the best choice seems SiO<sub>2</sub> and Au for overlay and metallic grating, respectively. Although metals with extremely large  $\rho$  and  $c_{44}$  such as W and Ta offer large  $K^2$ , they may not be acceptable for practical applications for their large electric resistivity.

## I. INTRODUCTION

High performance surface acoustic wave (SAW) devices have been widely used in telecommunication systems. Yet, as SAWs concentrate their energy close to the substrate surface, the air cavity between the substrate surface and package limits the SAW device for further downsizing and low-profiling.

For this problem, it has been known that applying piezoelectric boundary acoustic waves (PBAWs) [1-8] which propagate along the interface between two attached materials, one could completely eliminate the air cavity in SAW device packaging.

Various structures supporting PBAWs were proposed. For example, Kando *et al.* proposed a SiO<sub>2</sub> overlay/heavy grating electrode/rotated Y-cut X-propagating LiNbO<sub>3</sub> (YX-LN) substrate structure for developing PBAW devices.[4,5] They showed that the removed air cavity really makes the packaging most simple and enables the device size to be minimized, while the device fabrication process is very similar to that for conventional SAW devices.

In ref. [8], the authors discussed the structures supporting PBAWs using a simple model and predicted how to choose overlay and sandwiched layer materials as for non-leaky PBAWs with large electromechanical coupling factor  $K^2$ . The result suggested that the number of layers should be equal to or larger than three, in which the sandwiched layer was shown to be able to be replaced by a metallic grating as shown in [4,5]. It is also concluded that large  $K^2$  is obtained by combining a sandwiched layer (or metallic grating) having small shear bulk wave velocity  $V_{BS}$  and large mass density  $\rho$ , with the overlay having large  $V_{BS}$  and small  $\rho$ .

From this prediction, when rotated YX-LN is chosen as a piezoelectric underlay (substrate), it is expected that high velocity dielectric materials such as AlN, SiC and Si<sub>3</sub>N<sub>4</sub> may fulfill these requirements for the overlay in addition to SiO<sub>2</sub>. On the other hand, heavy metals such as Cu, Ag, Au, Mo, Ta and W seem to be possible candidates as a grating material used for the metallic grating.

Based on the above consideration, this paper investigates how the PBAW characteristics change with the combination of materials for the overlay and metallic grating.

The technique described in [6-9] was applied to the full-wave analysis of PBAWs propagating along the metallic grating sandwiched in between two semi-infinite layers. For the overlay, SiO<sub>2</sub>, AlN, SiC and Si<sub>3</sub>N<sub>4</sub> are examined while Cu, Ag, Au, Mo, Ta and W are for the metallic grating.

The results are in agreement with the qualitative discussion. That is, large  $K^2$  is obtained for the combination of an overlay having small  $\rho$  with a metallic grating having extremely large  $\rho$ . For example, when YX-LN is chosen as a substrate, the best choice seems to be SiO<sub>2</sub> and Au as overlay and sandwiched metallic grating materials, respectively. Although metals with extremely large  $\rho$  and stiffness constant  $c_{44}$  such as W and Ta offer larger  $K^2$ , they may not be acceptable for practical applications for their large electric resistivity.

---

This work is partly sponsored by TriQuint Semiconductors, Inc.

## II. SIMULATION

### A. Simulation Procedures

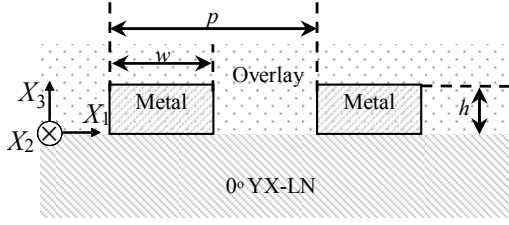


Fig. 1 Cross-sectional view of the structure

In the following analysis, YX-LiNbO<sub>3</sub> (0°-rotated YX-LN) was chosen as a substrate (underlay). Although the substrate rotation angle should be chosen appropriately to suppress spurious Rayleigh-type PBAWs [7], it does not give a significant impact on other properties of SH-type PBAWs.

Cross-sectional view of the structure used in the analysis is shown in Fig. 1. An infinitely-long IDT with the thickness  $h$ , the periodicity  $2p$  and the metallization ratio of 0.5 is placed at the boundary between the semi-infinite dielectric

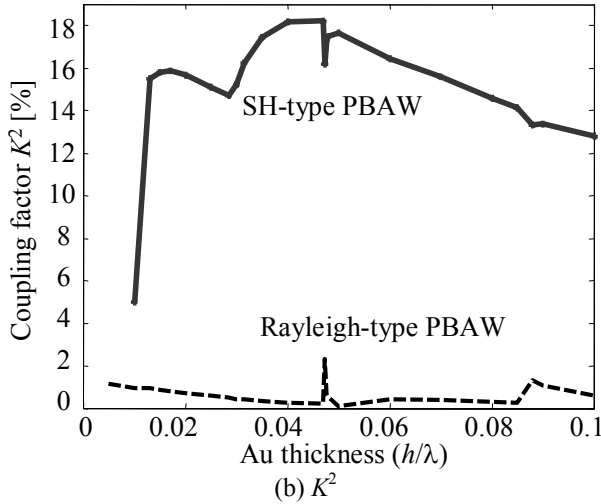
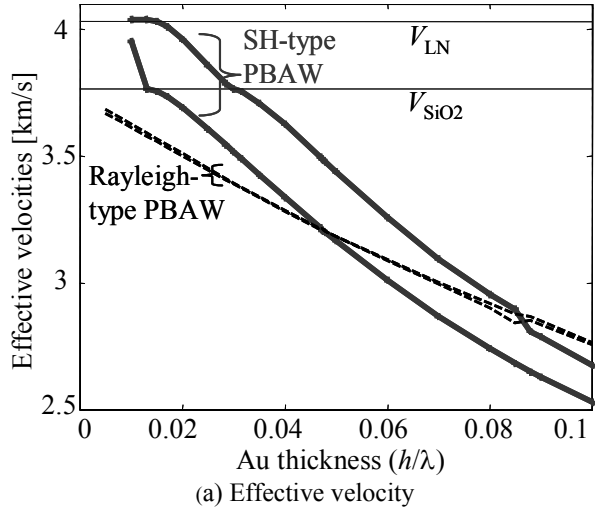


Fig. 2 PBAW properties in SiO<sub>2</sub>/Au/YX-LN structure.

overlay and the semi-infinite YX-LN underlay. Here the IDT electrodes, both sides of which are filled with the dielectric overlay, are assumed to behave as a sandwiched metallic grating. In the simulation, the IDT is assumed to be infinitely long along the  $X_2$  direction.

We calculate the input admittance  $\hat{Y}(f)$  of the IDT with infinitely long acoustic length as a function of the frequency  $f$  [6-9], from which the resonance and anti-resonance frequencies,  $f_r$  and  $f_a$ , are estimated for both SH- and Rayleigh-type PBAWs, respectively [10,11]. From  $f_r$  and  $f_a$ , the effective  $K^2$  is estimated by the following formula:

$$K^2 = (\pi f_r / 2 f_a) / \tan(\pi f_r / 2 f_a). \quad (1)$$

Fig. 2(a) shows, as an example, thus calculated effective velocities  $V_r (=2f_r p)$  and  $V_a (=2f_a p)$  as a function of the Au electrode thickness  $h$  when SiO<sub>2</sub> is chosen as an overlay. In the figure,  $V_{LN}$  is the slow shear bulk wave velocity in YX-LN (4,030 m/s), and  $V_{SiO_2}$  is for the shear bulk wave velocity in SiO<sub>2</sub> (3,766 m/s). We can see that the velocities decrease monotonically with an increase in  $h$ . When  $h$  is smaller than  $0.03\lambda$ , the PBAW velocity is greater than  $V_{SiO_2}$ . This means that  $h$  should be larger than this critical value  $h_c$  so that the corresponding PBAW is non-leaky.

Fig. 2(b) shows  $K^2$  calculated by Eq. (1). It is seen that  $K^2$  of the SH-type PBAW takes a relatively large maximum value  $K^2_{max}$  of 18.4% at  $h=0.04\lambda$ . There is a dip in  $K^2$  at  $h \approx 0.05\lambda$ . This is caused by the coupling between the SH-type and Rayleigh-type PBAWs, and it can be suppressed by properly adjusting the LN rotation angle [7].

### B. Results Analysis

At first, Au is chosen as a grating material, and the effect of the overlay material is investigated.

Fig. 3 shows the change in  $K^2$  with a choice of the overlay material, where only the non-leaky SH-type PBAW region is shown. Although the  $h$  dependence is similar to each other,

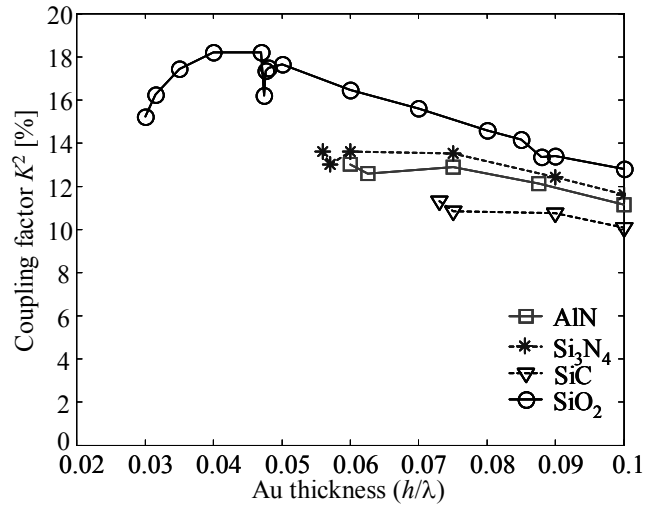


Fig. 3 Change in  $K^2$  for SH-type PBAW with overlay material

$K_{\max}^2$  of non-leaky PBAW and the thickness  $h_{\max}$  giving  $K_{\max}^2$  vary significantly with the material selection. It is seen that  $\text{SiO}_2$  gives the largest  $K_{\max}^2$  at the smallest  $h_{\max}$ , which is about 50% larger than the other materials.

TABLE I INFLUENCE OF OVERLAY MATERIAL SELECTION

Overlay material	$\text{SiO}_2$	$\text{Si}_3\text{N}_4$	$\text{AlN}$	$\text{SiC}$
Shear wave vel., $V_{\text{BS}}$ (m/s)	3,766	5,656	5,983	7,836
Mass density, $\rho$ ( $\text{kg/m}^3$ )	2,200	3,200	3,300	3,000
Stiffness, $c_{44}$ ( $10^{10}$ N/m $^2$ )	3.12	10.24	11.81	18.42
$h_c(\lambda)$	0.030	0.056	0.060	0.073
$h_{\max}(\lambda)$	0.047	0.056	0.060	0.073
$K_{\max}^2$ (%)	18.4	13.6	13.0	11.3

Table I compares the results with a few key material constants and parameters for the overlay. As can be seen, an increase in  $K_{\max}^2$  almost proportional to a decrease in  $\rho$ , while both  $h_{\max}$  and  $h_c$  increase with  $V_{\text{BS}}$ .

Thus  $\text{SiO}_2$  seems to be the best material for the overlay, although the resulting PBAW velocity is somewhat slow, because it should be slower than  $V_{\text{BS}}$  (3,766 m/s) to be non-

leaky. In addition,  $\text{SiO}_2$  may improve the temperature stability as well.

Next,  $\text{SiO}_2$  is chosen as the overlay material, and the effect of the grating electrode material is investigated.

Fig. 4 shows the change in  $K^2$  with  $h$ , where only the non-leaky SH-type PBAW region is shown. Although the  $h$  dependence is similar to each other,  $K_{\max}^2$  of non-leaky PBAW and  $h_{\max}$  vary significantly with the material selection.

Table II compares the results with a few key material constants and parameters for the sandwiched metallic grating. Although the dependences of  $K_{\max}^2$ ,  $h_c$  and  $h_{\max}$  upon the material parameters are complicated, they generally possess the following tendencies;  $K_{\max}^2$  increases with  $\rho$  and  $c_{44}$ , and  $h_c$  and  $h_{\max}$  decreases with an increase in  $\rho$ . Metals having extremely large  $\rho$  and  $c_{44}$  such as W and Ta offer larger  $K^2$  than Au and Cu. Because of their poor electric conductivity, however, W and Ta may not be acceptable for practical applications.

In Fig. 4, there are some abrupt changes in  $K^2$ , which are caused by the coupling between the SH-type and Rayleigh-type PBAWs. In ref. [7], the authors indicated that the coupling can be avoided by properly adjusting the rotation angle of the substrate. To make sure of this, the calculation was carried out by changing the rotation angle of LN substrate.

Fig. 5 shows the result. It is clearly seen that the abrupt change in  $K^2$  caused by the coupling is sufficiently suppressed by changing the rotation angle from  $0^\circ$  to  $-5^\circ$ , and that  $K^2$  larger than 18% is achievable in a wide range of  $h$ .

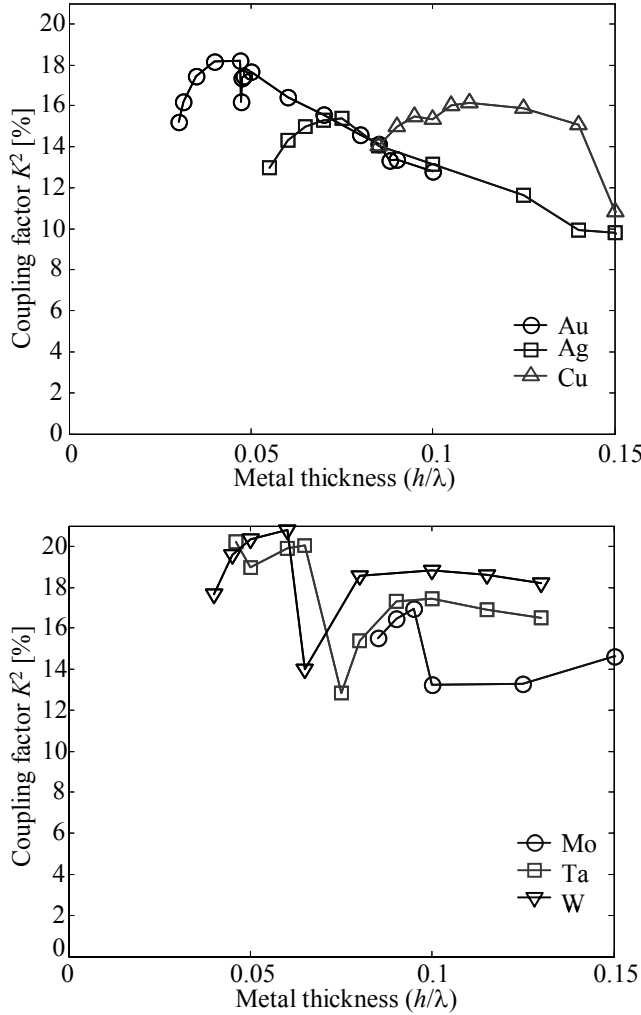


Fig. 4 Variation of  $K^2$  with the metal thickness in  $\text{SiO}_2$ /metal grating/YX-LN structure

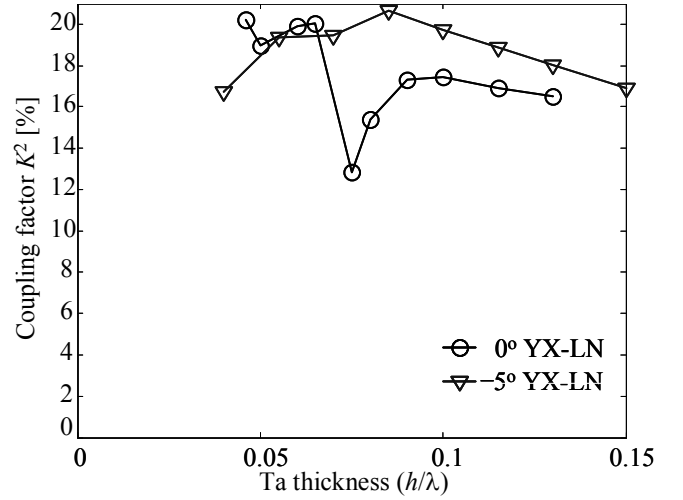


Fig. 5 Variation of  $K^2$  with the Ta thickness in  $\text{SiO}_2$ /Ta/rotated YX-LN structure

### III. CONCLUSION

In this paper, we applied the full-wave analysis to the overlay/metallic grating/substrate structure supporting PBAWs, and discussed how the PBAW characteristics change with the combination of overlay and metallic grating materials.

It was shown that large  $K^2$  is obtained when materials having small  $\rho$  and materials having extremely large  $\rho$  and  $c_{44}$  are chosen, respectively, for an overlay and a metallic grating. In addition, increased  $\rho$  of sandwiched grating materials is effective in making both  $h_c$  and  $h_{\max}$  relatively small.

In conclusion, when YX-LN is chosen as a substrate, one of the best choice seems to be  $\text{SiO}_2$  and Au as overlay and sandwiched grating materials, respectively. Although metals with extremely large  $\rho$  and  $c_{44}$  such as W and Ta offer large  $K^2$ , they may not be acceptable for practical applications for their large electric resistivity.

#### ACKNOWLEDGMENT

It is our pleasure to thank Dr. Benjamin P. Abbott of TriQuint Semiconductor, Inc. for his fruitful suggestions and discussions.

#### REFERENCES

- [1] C.Maefeld and P.Tournois: "Pure shear elastic surface wave guided by the interface of two semi-infinite media," *Appl. Phys. Lett.*, vol. 19, pp. 117-118, 1971.
- [2] T.Yamashita, K.Hashimoto and M.Yamaguchi, "Highly piezoelectric shear-horizontal-type boundary waves," *Jpn. J. Appl. Phys.*, vol. 36, no. 5B, pp. 3057-3059, 1997.
- [3] M.Yamaguchi, T.Yamashita, K.Hashimoto and T.Omori, "Highly piezoelectric boundary waves in  $\text{Si/SiO}_2/\text{LiNbO}_3$  structure," in *Proc. IEEE Freq. Contr. Symp.*, 1998, pp. 481-484.
- [4] H.Kando, D.Yamamoto, M.Mimura, H.Tochishita and M.Kadota, "RF filter using boundary acoustic wave," in *Proc. IEEE Ultrason. Symp.*, 2006, pp. 188-191.
- [5] H.Kando, D.Yamamoto, H.Tochishita and M.Kadota, "RF filter using boundary acoustic wave," *Jpn. J. Appl. Phys.*, vol. 45, no. 5B, pp. 4651-4654, 2006.
- [6] K.Hashimoto, T.Omori and M.Yamaguchi, "Extended FEM/SDA software for characterising surface acoustic wave propagation in multi-layered structures," in *Proc. IEEE Ultrason. Symp.*, 2007, pp. 711-714.
- [7] Y.Wang, K.Hashimoto, T.Omori and M.Yamaguchi, "Full-wave analysis of piezoelectric boundary waves propagating along metallic grating sandwiched in between two semi-infinite layers," in *IEEE Trans. Ultrason. Ferroelec. Freq. Cont.*, vol. 56, no. 4, pp. 806-811, 2009.
- [8] K.Hashimoto, Y.Wang, T.Omori, M.Yamaguchi, M.Kadota, H.Kando and T.Shibahara, "Piezoelectric boundary acoustic waves: their underlying physics and applications," in *Proc. IEEE Ultrason. Symp.*, 2008, pp. 999-1005.
- [9] Y.Wang, K.Hashimoto, T.Omori and M.Yamaguchi, "A full-wave analysis of surface acoustic waves propagating on a  $\text{SiO}_2$  overlay/metal grating/rotated YX- $\text{LiNbO}_3$  substrate structure," *Jpn. J. Appl. Phys.*, [to be published]
- [10] K.Hashimoto, *Surface Acoustic Wave Devices in Telecommunications: Modeling and Simulation*. Springer, Chapter 7 and 8, 2000, pp.191-270.
- [11] K.Hashimoto, "Simulation of surface acoustic wave devices, review," *Jpn. J. Appl. Phys.*, vol. 45, no. 6B, pp. 4423-4428, 2006.

TABLE II INFLUENCE OF SELECTION OF METAL GRATING MATERIAL

Metal	Au	W	Ta	Ag	Mo	Cu
Shear wave vel., $V_{\text{BS}}$ (m/s)	868	2,642	2,039	1,188	3,495	2,326
Mass density, $\rho$ ( $\text{kg/m}^3$ )	19,300	19,250	16,690	10,490	10,280	8,930
Stiffness, $c_{44}$ ( $10^{10} \text{ N/m}^2$ )	1.445	16.06	6.94	1.48	12.56	4.83
Electrical conductivity ( $10^6 \text{ S/m}$ )	45.2	18.9	7.63	63.01	18.7	59.6
$h_c(\lambda)$	0.03	0.04	0.046	0.055	0.085	0.085
$h_{\max}(\lambda)$	0.047	0.06	0.046	0.075	0.095	0.11
$K_{\max}^2(\%)$	18.2	20.8	20.2	15.4	17.0	16.2